Microstructural and geo-mechanical study on bio-cemented sand for optimization of MICP process

Donovan Mujah[1]; Liang Cheng Ph.D.[2] and Mohamed A. Shahin, F.ASCE[3]

[1]PhD Scholar, Department of Civil Engineering, Curtin University, Australia

[2] Corresponding author: Professor, School of Environment and Safety Engineering, Jiangsu University, China. Email: ClCheng@ujs.edu.cn

[3]Associate Professor, Department of Civil Engineering, Curtin University, Australia.

ABSTRACT:

Limited research has been reported on strength improvement of bio-cemented soils in relation to crystal patterns of microbial induced calcite precipitation. In this study, sand samples were treated under the co-effect of different bacterial culture (BC) and cementation solution (CS) concentrations, to evaluate the optimum BC and CS combination that yields the highest soil strength. It was found that for lower CS condition (0.25 M), higher BC produced stronger samples, whereas for higher CS condition (0.5 M or 1 M), lower BC was more dominant in improving the soil strength. This can be attributed to the effectively precipitated $CaCO_3$ crystals, which were in rhombohedral shape and large size, and were concentrated at the soil pore throat rather than deposited on the individual sand grain surface. This finding was confirmed with the scanning electron microscopy (SEM) analysis. The strength and permeability of the optimized bio-cemented samples were also compared with sand samples treated with ordinary Portland cement (OPC). The optimized bio-cemented sand provided higher strength and permeability than those obtained from the samples treated with similar content of OPC at curing period of 28 days.

Introduction

The recent advances in soil stabilization using microbial induced calcium carbonate ($CaCO_3$) precipitation (MICP) technique has been reported by Mujah, et al. (2016b). For geotechnical applications, microbial grouting is mostly utilized to strengthen soils by means of increasing soil strength and stiffness through the bio-mineralization of $CaCO_3$ crystals that act as a cementing agent, binding soil particles together inside the soil matrix (Cheng, et al., 2013). Another potential of microbial grouting is through the concept of bio-clogging, as a result of the agglomeration of the $CaCO_3$ crystals in the soil pore throats, thus, controlling the water flow in the porous media to reduce the hydraulic conductivity of the bio-clogged soils (Ivanov and Chu, 2008).

The mechanical performance of MICP stabilized soils largely depends on the microstructure of the precipitated CaCO3 crystals, which are affected by various chemical, environmental and physical parameters. Studies by Chu, et al. (2013), Al Qabany, et al. (2012), Mortensen, et al. (2011) and Martinez, et al. (2013) discussed the treatment conditions to achieve an overall MICP treatment process efficiency in terms of the uniformity of $CaCO_3$ precipitation. It was suggested that the use of lower concentrations of cementation solution (CS) and bacterial culture (BC) would result in better distribution of $CaCO_3$ precipitation, particularly at lower cementation levels. Cheng, et al. (2013) demonstrated that the bio-cemented soils treated at partially saturated conditions resulted in higher strengths than those achieved under full saturation conditions, due to the more CaCO3 crystals precipitated at the contact points between the sand grains. In other words, alteration of the $CaCO_3$ crystals precipitation patterns can have significant effect on the mechanical response of bio-cemented soils.

Earlier studies found in the literature concluded that the alteration of the cementation solution concentrations (in terms of different combinations or the equimolar amount of urea and calcium) would result in uniformly distributed $CaCO_3$ crystals, leading to enhanced bio-cemented sand strength and reduction in hydraulic conductivity (Al-Thawadi and Cord-Ruwisch, 2012, Al Qabany and Soga, 2013, Jiang and Soga, 2017, Jiang, et al., 2016, Mujah, et al., 2016a, Okwadha and Li, 2010, Whiffin, 2004, Yasuhara, et al., 2012). Interestingly, Cheng, et al. (2013) found that the strength of bio-cemented sand may not be directly influenced by the $CaCO_3$ distribution homogeneity but rather by the precipitation of the effective $CaCO_3$ crystals defined as the "bridging" crystals that precipitate at the contact points between the sand particles. Furthermore, it has been suggested that the precipitation patterns of the $CaCO_3$ crystals are mainly governed by the interplay between the BC and CS concentrations (Cheng, et al., 2017).

Previously, Al Qabany, et al. (2012) and Martinez, et al. (2013) discussed several factors affecting the overall process efficiency of MICP treatment such as the CS concentrations, retention times, input rates, flow rates, flow directions, and formulations of biological and chemical amendments. It was noted that the main purpose of such studies was to achieve the $CaCO_3$ cementation uniformity. The present study however focuses on the precipitation of the effective $CaCO_3$ crystals that link two or more individual sand particles together in the soil matrix by means of particle binding mechanism. Also, the optimization procedure presented herein refers solely to the condition at which the $CaCO_3$ crystals are precipitated and contributed to the particle binding.

Although Shahrokhi-Shahraki, et al. (2015) considered different BC and CS concentrations in their attempt to elucidate the strength and hydraulic properties of bio-cemented sand, their results did not appear to be a comprehensive representation of the whole cementation spectrum (only weak cemented samples with the highest UCS value of 240 kPa was considered). Furthermore, the link between the different BC and CS concentrations with the structure of induced crystals, and the corresponding mechanical strength has not been clearly revealed due to the limited samples conducted. In order to fairly assess the contribution of different BC and CS concentrations, a series of MICP treated samples that correspond to weak, medium and strongly cemented conditions must be considered. The current study aims to provide a deeper understanding of the microstructural characteristics of the various $CaCO_3$ crystals precipitation patterns, to establish the relationship between the precipitated $CaCO_3$ crystals structure as a result of the interaction between the bacteria and cementation solution concentrations with the corresponding strength of bio-cemented sand post treatment. The optimum combination of bacteria and cementation solution concentrations that produces the most effective $CaCO_3$ crystals was also highlighted. For the purpose of this study, the efficacy of the $CaCO_3$ crystals was measured in terms of the strength gained per mass of $CaCO_3$. The observed relationship between the different $CaCO_3$ precipitation patterns and the corresponding strength of bio-cemented sand obtained from the current study can have implications for the use of MICP for soil treatment in field applications.

Materials and Methods

Soil type

Natural silica sand obtained from Cook Industrial Minerals Pty Ltd, Western Australia was used in the present study. The basic soil physical properties of the sand used are given in Table 1. According to the Unified Soil Classification System (USCS), the sand used is classified as poorly graded sand (SP).

Bacteria culture and cementation solution

Bacillus sp. bacteria isolated from a previous work carried out by Al-Thawadi and Cord-Ruwisch (2012) were used in the current study. The growth medium consisted of 20 g/L yeast extract, 0.17 M ammonium sulphate and 0.1 mM nickel chloride with a final pH value adjusted to 9.25. Then, the isolated strain was inoculated into the sterilized growth medium and shaken inside a water bath for 48 h at a constant temperature of 30°C. After 72 h of incubation, the bacteria were harvested and stored at 4°C storage prior to use. The optical density (OD_{600}) of the harvested bacteria culture varied between 2 – 2.5. It is worthwhile to mention that the OD_{600} value shows a good linear relationship with the urease activity of the bacterial cultures collected between the exponential growth phase and early stationary phase. The raw bacterial culture was either concentrated (by centrifuge) or diluted (by tap water) to gain a specific urease activity. The recipe for the BC and CS used in the experiments was listed in Table 2. It should be noted that 1 U/mL of urease means an amount of urease enzyme contained in 1 mL of culture used to hydrolyze 1 μmol of urea per minute. The urease activity was determined from the ammonia production rate, which was determined by the Nessler's method (Cheng et al. 2016). The cementation solutions used in the current study consisted of equimolar of urea and calcium chloride anhydrous. A total of three final CS concentrations were considered in the current study (i.e., 0.25 M, 0.5 M, and 1 M). Higher CS concentration above 1.5 M was found to result in a reduced $CaCO_3$ content, according to Whiffin (2004). No less than 0.25 M CS concentration was adopted since more CS treatment cycles are required to achieve adequate amount of $CaCO_3$ precipitates.

Specimen preparation

Polyvinyl chloride (PVC) column with diameter 45 mm and height 150 mm was vertically cut into half and glued together using silicon glue to allow for the bio-cemented column extraction after the MICP treatment. The top part (inlet) of the column was affixed to a peristaltic pump with a constant flow rate of 1 L/h to inject reagents into the PVC column while the bottom part (outlet) was connected to a U-shape tubing. To expedite the spread of solution and avoid the sand particles from being flushed out during the treatment cycles, scour pads (pore size less than 1 mm) and 10 mm thick coarse sand layers (grain size 1.18-2.36 mm) were placed on both ends of the column. The sand used was compacted into 3 consecutive layers, ensuring that each layer achieved 95% of the maximum dry density to maintain experiment consistency. The PVC column was fully saturated by an upward flow method with tap water for 24 h. Then, the MICP treatment was conducted using the downward flow injection method. The water level in the external U-type tubing attached to the outlet of the PVC column was maintained to be on par with the inlet cap to maintain fully saturated condition during MICP treatment.

After 24 h, the MICP reagents were injected into the PVC column following a modified two-phase injection strategy (Cheng and Cord-Ruwisch, 2014, Martinez, et al., 2013), as follows. In the first phase, half void volume of BC and half void volume of CS were injected alternately into the PVC column, followed by 24 h of waiting period to ensure fixation of the bacteria cells onto sand particles. Then, a full void volume of CS was injected and left to cure for another 24 h (except elsewhere stated) to allow for $CaCO_3$ precipitation. This treatment cycle was repeated several times to gain different levels of cementation. After treatment was completed, the soil samples were flushed with tap water to remove all soluble salts. At each treatment injection, the ammonia content and bacterial activity of the effluent were collected and measured to calculate the chemical conversion efficiency of each treatment. The drainage of the pore solution was driven by injecting new bio-cementation solution from the top of the sand column, this down-flow injection provided minimum disturbance to the soil sample.

Optimum condition for effective $CaCO_3$ precipitation

In order to evaluate the optimum combination of BC and CS concentrations that produces the most effective $CaCO_3$ crystals, a series of different BC and CS concentrations, as listed in Table 2, were used in the experiment. Also, the effect of the number of CS flushes on the ammonia conversion efficiency of each treatment, which is defined as the percentage of injected urea that was converted to ammonia, of the bio-cemented samples was studied. For the purpose of this study, the following two items are valid: (1) only reagents that were able to sustain at least 50% efficiency (i.e. urea to ammonia conversion) are considered; and (2) one flush of CS is equivalent to 24 hours reaction time. The number of CS flushes is of interest in the current study in order to determine the supplied BC upon repeated injections of CS per treatment cycle.

Strength test

Unconfined compressive strength (UCS) tests were conducted on all treated soil specimens having a constant diameter-to-height ratio of 1:2, which were crushed with an axial load rate of 1 mm/min. The strength of the optimized bio-cemented samples was compared with those obtained from the conventional soil improvement method using mixtures of sand (350 g) and various proportions of ordinary Portland cement (OPC) (ranging from 2-10%) including 45 mL of water. The mixtures were poured into the PVC columns having the same dimensions used for the bio-cemented samples, and a vibration was applied to circumvent any air bubbles entrapment inside the mixtures. The mixtures were submerged inside the water bath at the room temperature for 7 and 28 days to cure prior to UCS measurements. It should be noted that the specimen preparation procedure is rather different in the MICP and OPC treatments; the MICP requires only flushing while the OPC needs thorough mixing. The ultimate goal of this study is to compare the outcomes of the MICP treated soil with OPC treated soil under their optimum treatment conditions.

$CaCO_3$ content determination

In order to determine the $CaCO_3$ content (excluding the unbounded free calcite in the soil pore space which was flushed out by water after treatment) of the bio-cemented sand samples, the crushed cemented samples were oven dried in 105°C for 24 h prior to the $CaCO_3$ content test. A mass of 1 g of dried soil taken at various degrees of cementation was mixed with 2 mL of 2 M hydrochloric acid, at which the volume of the carbon dioxide gas produced by the reaction was measured using a U-tube manometer under standard conditions of 25°C at 1atm (Whiffin, et al., 2007). This process was repeated at least three times for each sample.

Microstructural analysis

The link between the $CaCO_3$ crystals microstructural characteristics and the corresponding strength of bio-cemented sand post-treatment was investigated using scanning electron microscopy (SEM - MIRA TESCAN 3). Only the intact small sand chunks were used for the SEM analysis, therefore, the bonding and microstructure of the intact sand chunks remained undisturbed. The bonding behavior between the host grain and the structure of the $CaCO_3$ crystals, as well as the evolution of the effective $CaCO_3$ crystals morphology were examined.

Presentation of Results

Effect of different treatment combinations towards UCS

The effects of different BC concentrations on the strength of the bio-cemented samples at various CS concentrations are shown in Fig. 1. It can be observed that for all BC concentrations, the UCS increases almost exponentially with the increase of $CaCO_3$ content, regardless of the CS concentrations. It can also be seen that the strength response of bio-cemented samples differs for different CS concentrations. For example, at lower CS concentration (i.e., 0.25 M), the samples treated with higher BC concentrations were more effective in terms of the strength improvement per the amount of calcite formed. Interestingly, almost similar trend of strength development was noted at 0.5 M CS concentration, regardless of the BC concentrations. In contrast, at higher CS concentration (particularly at 1 M CS condition), the samples treated with lower BC concentrations were more effective. It can also be observed that the samples treated at high BC concentration (i.e., 32 U/mL) together with low CS concentration (i.e., 0.25 M) were the most effective, whereas the samples treated with a combination of high BC concentration (i.e., 32 U/mL) and high CS concentration (i.e., 1 M CS) showed the lowest strength improvement.

The microstructural observations through the SEM analysis carried out on the bio-cemented samples for the most effective strength improvement (i.e., high BC: 32 U/mL and low CS: 0. 25M) as well as the least effective strength improvement (i.e., high BC: 32 U/mL and high CS: 1 M) were presented in Fig. 2. It can be seen from Fig. 2(a & b) that the agglomeration of large clusters of $CaCO_3$ crystals (approximately > 20 μm) under high BC and low CS concentrations linked two or more sand grains together, hence, contributing to the effectiveness of the strength gained. The precipitation of large $CaCO_3$ crystals would increase the area of contact for greater shearing resistance, thus, contributing to high UCS value. However, it should be mentioned that the relative size between the $CaCO_3$ crystals and sand particles are more important than the absolute size of the crystals themselves, as the crystals need to be large enough to fill in the contact points of the different sand grain sizes.

Fig. 2(c & d) shows the precipitation of relatively smaller $CaCO_3$ crystals (approximately < 10 µm) for combination of high BC and CS concentrations.

The different sizes of the $CaCO_3$ crystals formed in this study may be attributed to the competition between the crystal growth and crystal nucleation as a result of the interplay between the CS and BC concentrations. Gandhi, et al. (1995) reported that the competition would occur if the nucleation of new crystals triumphs over the growth rate of the existing ones. In the case of high BC and low CS concentrations, a high number of bacterial cells were introduced into the soil samples and attached to the sand grain surface. In principle, a high number of bacterial cells would provide the abundance of nucleation sites in the soil matrix (Cheng, et al., 2017). In the presence of CS, the urea hydrolysis reaction is triggered to produce CO_3^{2-} ions, which were then mainly consumed by the nucleation of new $CaCO_3$ crystals rather than the growth of the existing ones. Initially, this leads to abundance of the small $CaCO_3$ crystals but with continuous supply of low CS concentration, the numerous small crystals would develop to grow larger in size, as shown in Fig. 2(b).

The size of the $CaCO_3$ crystals precipitated using high BC and CS concentrations was comparatively smaller (approximately 10 µm) compared to the crystals formed under high BC and low CS concentrations, as shown in Fig. 2(d). In both conditions, the amount of BC concentration was fixed to 32 U/mL, and the only difference was on the CS concentration. It has been demonstrated that the CS concentration affects the super-saturation condition (difference between the actual concentration and solubility concentration) of the environment that favors MICP process (Bosak and Newman, 2005), which is usually affected by the Ca^{2+} and CO_3^{2-} ions sources from the $CaCl_2$ and $CO(NH_2)_2$. The higher the super-saturation, the greater the nucleation rate of $CaCO_3$ crystals, resulting in formation of small crystals (Al-

Thawadi and Cord-Ruwisch, 2012). The presence of smaller $CaCO_3$ crystals leads to the least strength improvement in the combination of 32 U/mL BC and 1 M CS.

The correlation between the shear strength of bio-cemented sand and amount of $CaCO_3$ content has been investigated previously by Fujita et al. (2000), Whiffin et al. (2007) and Okwadha and Li (2010), concluding that the amount of CaCO3 content may not necessarily contribute to the soil strength improvement. Cheng et al. (2013) and Cheng et al. (2017) showed how sand grains coated with $CaCO_3$ crystals have less strength efficiency than the accumulation of $CaCO_3$ crystals at the contact points (i.e., effective $CaCO_3$ crystals). The current study confirms the efficacy of the strength improvement by the effective $CaCO_3$ crystals (rhombohedral-shaped, large and concentrated at soil pore throat). The accumulation of the effective $CaCO_3$ layers that adhere to the initial $CaCO_3$ precipitates would increase the size of the $CaCO_3$ crystal as more low concentrated reagent was supplied, thus, increasing the total area of contacts between the $CaCO_3$ crystals and the host sand grains.

Effectiveness of MICP on treated samples

Based on the findings obtained from the treatment strategy employed in this study, it was clearly that the different $CaCO_3$ precipitation patterns are governed by the combined concentrations of BC and CS supplied during MICP treatment. Therefore, it is imperative to study the chemical conversion efficiency of the repeated injections of CS per injection of BC in order to produce a more cost-effective MICP process for field applications.

Fig. 3 shows the effect of the number of CS flushes on the chemical conversion efficiency (CCE) of the MICP process. Only the extreme case involving the lowest BC (8 U/mL) [Fig. 4(a)] and the highest BC (32 U/mL) [Fig. 3(b)] concentrations were presented in the current paper to differentiate the effect of the in-situ urease activity towards the chemical conversion efficiency. Based on Fig. 3(a & b), it can be seen that regardless of the BC concentration, the CCE of each treatment diminishes with the number of CS treatments. Also, the accumulative mass of $CaCO_3$ precipitates (obtained from the chemical conversion efficiency) of each condition was calculated. It is shown from Fig. 3 that the decreasing CCE is related to the total amount of the produced $CaCO_3$. The observed gradual decrease in the CCE after each flush, which is in line with van Paassen, et al. (2010), indicates the loss of urease activity which is possibly due to the bacterial cell encapsulation, elution of cells or cells death or lysis. The optimum number of CS flushes is crucial for field application since it provides guidelines in determining the number of CS injection required to completely consume the supplied BC in each treatment cycle. It can be seen form Fig. 3 that higher BC concentration (i.e., 32 U/mL) can sustain higher number of CS flushes, whereby the chemical conversion efficiency was higher than 50% comparing to that of the lower BC concentrations. The higher number of CS flushes obtained in the 32 U/mL BC concentration can be attributed to the higher amount of bacteria cells existed in the BC solution. The amount of bacteria cells available in the MICP environment would allow the continuity of the MICP process. It is worth noting that Cheng, et al. (2016) and Feng and Montoya (2016) recommended multiple injections of bacteria to recover the in-situ urease activity and achieve a high level of cementation to continue the MICP process. Also, the recovery of the loss of urease activity during the MICP process can be achieved by the in-situ enrichment of ureolytic bacteria via providing a specific growth medium (Gomez, et al., 2016) or through the reintroduction of the ex-situ cultivated bacterial culture.

Evolution of the effective $CaCO_3$ crystals precipitation via SEM images

To study the morphology of the $CaCO_3$ crystal precipitates and their evolution as a function of the BC and CS injections over time, the specimens taken from the sand column after one, two and four times of CS treatment were prepared for SEM analysis. The precipitation pattern of the effective $CaCO_3$ crystals will be deliberated at length in the current study. It should be noted that the combination of the reagents used in this study to produce the effective $CaCO_3$ crystals was based on the optimum result discussed in the preceding section. Fig. 4 shows the precipitation and evolution of the effective $CaCO_3$ crystals formation found in this study. Bacteria colonies attachment onto the sand grain surface encourages the formation of nucleation site for the birth of new $CaCO_3$ crystals in the soil matrix. Subsequent flushing of CS into the sample would induce the precipitation of metastable primary spherical precipitates, known as vaterite circled in red in Fig. 4(a & b) as previously shown by van Paassen (2009) and Al Qabany, et al. (2012). Also, the transformation of the primary circular crystal into the more stable secondary rhombohedral shaped $CaCO_3$ is captured in Fig. 4(c & d). This observation is in line with the transition phase reported by Terzis, et al. (2016), which observed similar $CaCO_3$ crystals transformation.

The first supply of CS would initially introduce Ca^{2+} ions into the bio-cemented samples and contributing towards the birth of new $CaCO_3$ crystals. In its stable form, further supply of CS together with the deposition of CO_3^{2-} ions from urea hydrolysis by bacteria onto the $CaCO_3$ crystal surface would increase the size of the $CaCO_3$ crystals (Anbu, et al., 2016, Park, et al., 2014). Unlike previously thought by (Al Qabany and Soga, 2013, DeJong, et al., 2010), the crystal growth in the current study possibly stems from the agglomeration of the single crystals (observed after the 1st and 2nd treatment) creating mesocrystals (after the 4th treatment) which eventually form the effective $CaCO_3$ crystals [Fig. 4(c & d)].

Comparison between MICP and OPC treated samples

In order to further verify the optimized strength and permeability of the bio-cemented sand samples, a series of MICP treated samples were produced and compared with those obtained from the conventional method of chemical soil stabilization using ordinary Portland cement (OPC) cured at 28 days. Figs. 5 and 6 show comparison of the stress-strain relationships of the MICP and OPC treated sands at various contents of cementing agent. It can be derived that the increase in $CaCO_3$ or cement content increases the peak strength of both samples, as one would expect. Based on the results of Fig. 5, the peak strength recorded for the MICP treated sand at 4%, 6%, 8%, and 10% $CaCO_3$ were found to be 850 kPa, 1200 kPa, 2200 kPa, and 4100 kPa, respectively. Based on the results pf Fig. 6, the peak strength documented for OPC treated sands at 4%, 6%, 8%, and 10% cement contents were found to be 500 kPa, 1100 kPa, 1500 kPa, and 3000 kPa, respectively. Also, it is noted that at < 6% cement content, the OPC treated samples exhibit relatively ductile behavior compared to the behavior of bio-cemented samples, and this is in line with the findings obtained by Schnaid, et al. (2001) and Ismail, et al. (2002b).

Fig. 7 shows the UCS and permeability results of the sand samples treated with the optimized bio-cement effective $CaCO_3$ and OPC treated with 2-10% cement content at 28 days of curing. It can be seen that the optimized bio-cemented samples have higher strength compared to the OPC treated samples at all cementation levels. For example, a mixture of the optimized bio-cemented sample has UCS value of 1550 kPa (at 6% $CaCO_3$ content) while the OPC sample treated with 6% cement has UCS value of 650 kPa (at 7 days) and 1210 kPa (at 28 days). The permeability of the optimized bio-cemented samples is significantly higher than that of the OPC treated samples at all cementation levels. For instance, at 6% cement content, the permeability of the OPC treated sample is considerably reduced to 98%, while the optimized bio-cemented sample retained about 50% of the initial permeability. At cement content > 8%, the OPC treated sample would act as a very poor drainage material having a permeability value of less than 1×10^{-5} m/s.

The increased strength and significant loss of permeability in the OPC treated samples are due to the cement hydration process, which occurs up to 28 days after the initial reaction between the cement and the soil (Achal, et al., 2015, Mujah, 2016, Nakarai and Yoshida, 2015). According to Cheng, et al. (2013), the cement hydration process produces water insoluble hydrates (i.e., calcium silicate hydrate C-S-H gel). The formation of the gel-like structure binds the sand particles together, leading to an increase in the strength and stiffness of the OPC treated sand. It should be noted that the OPC cementation process presented in the present study is representative of the traditional ground improving technique for soil stabilization using chemical additives (e.g. cement, gypsum, or lime). Observation into the microscale level of the OPC treated samples reveals that the C-S-H gel [Fig. 8(a-b)] would occupy most of the pore space, hence, limiting the permeability of the cemented material. Unlike the formation of the C-S-H structure, the precipitated $CaCO_3$ did not completely fill the gaps between the sand grains, hence, allowing passage for liquid transfer in the soil matrix [indicated by the red lines in Fig. 8(c). The $CaCO_3$ crystals in their solid form would cause smaller volume change while achieving stronger and stiffer post treatment mechanical responses compared to the C-S-H gel hydrates.

Discussion

The findings obtained from this study suggest that different $CaCO_3$ precipitation patterns can be engineered from the interplay of different BC and CS concentrations through MICP treatment, which result in different macroscale strength responses. In general, effective

$CaCO_3$ crystal precipitation pattern emerged (i.e., large, rhombohedral-shaped and clustered crystals). The $CaCO_3$ crystal precipitation pattern, including the relative size between crystals and sand particles which could effectively fill in the gaps between the sand particles, greatly impacts the target application of bio-cementation in the field because it affects the strength of bio-cemented soils by means of the load transfer mechanism inside the soil matrix, which depends on the size of the contact area, linked by the precipitated $CaCO_3$ crystals (Ismail, et al., 2002a). Depending on the shape, size and distribution of the precipitated $CaCO_3$ crystals near the soil pore throats, it can influence the flow properties of the porous media, leading to treatment homogeneity (Al Qabany, et al., 2012). It should also be noted that in addition to the amount of effective $CaCO_3$ crystals formed, the spatial uniformity of the overall microbially induced $CaCO_3$ precipitates would also be a critical factor controlling the ultimate soil strength.

In civil engineering applications such as transportation subgrades and embankments, the ability to apply MICP technique that can produce high efficacy $CaCO_3$ crystals (effective $CaCO_3$ precipitation) is desirable to minimize cost. The current study suggests that with the combination of high BC and low CS, an effective $CaCO_3$ precipitation could be produced. The formation of effective $CaCO_3$ would increase the strength and stiffness of treated foundations for transportation subgrades and embankments, while maintaining a fairly high permeability characteristic.

In terms of the comparison of strength improvement and permeability conducted for the MICP and OPC treated sands, it was shown that the optimized bio-cemented sand that features the precipitation of effective $CaCO_3$ crystals performed better in terms of strength improvement when compared to OPC treated sands at 28 curing days. This is mainly attributed to the precipitation of the effective $CaCO_3$ crystals with specific characteristics such as the presence of large, rhombohedral shaped and clustered $CaCO_3$ minerals rather than the production of the C-S-H gel in OPC treated sand that contributed towards the sand grains binding. The use of OPC treated sand is favored than the bio-cemented sand for field application when the effect of permeability reduction is important due to the fact that the C-S-H gel structure developed in the OPC treated sand mostly occupying the pore space between the sand grains, thus, limiting the liquid passage way. In contrast, if the permeability retention characteristic is preferred, the use of the optimized bio-cemented sand would be the way forward due to its ability to retain up to 50% of the initial permeability, even at high cementation level.

It is worthwhile to point out some limitations of the current optimization to achieve the effective $CaCO_3$ crystals precipitation, including: (1) different BC concentrations used were harvested from one single bacterium source (e.g., *Bacillus sp.*); (2) different CS concentrations used were based on equimolar concentrations (1:1) of urea that sourced the CO_3^{2-} ions and $CaCl_2$ that sourced the Ca^{2+} ions; and (3) injection strategy used based on two-phase injection approach. It is postulated that using different type of ureolytic bacteria with either higher or lower BC concentrations and different non-equimolar concentrations of CS compared to the current strain might yield different results because in order to achieve the same urease activity used in the current study, different amount of biomass is required, resulting in different number of nucleation sites and thus, affecting the $CaCO_3$ crystals precipitation patterns. Different injection strategy might cause various outcomes of bacteria and CS distribution within the sand columns, hence, resulting in various mechanical performances. The conclusions of the current research might not be applicable to other types of sands (e.g., calcareous), which have different mineralogy properties. This is because the surface properties of the soil grain would have significant effect on the characteristics of the $CaCO_3$ precipitates, thus, affecting the bonding behavior and ultimate mechanical performance of treated soils. However, the methodology developed in the current study can be employed on other types of soils.

Conclusion

This paper has shown the influence of the co-effect of BC and CS concentrations on the different $CaCO_3$ precipitation patterns and their relationship with the mechanical behavior of the bio-cemented sand. Based on the findings obtained from the treatment strategy employed in this study, the combination of 32 U/mL BC and 0.25 M CS resulted in the highest soil strength. Samples examined under the SEM indicated that effective $CaCO_3$ (i.e., large, rhombohedral-shaped and mainly concentrated at the soil pore throats) crystals could be produced through the combination of high BC (32 U/mL) and low CS (0.25 M) concentrations. This type of $CaCO_3$ precipitates significantly improved the soil strength and stiffness while maintaining sufficient permeability characteristic of the bio-cemented sand, thereby, would benefit the soil stabilization in civil engineering projects such as transportation subgrades and embankments.

The optimization of the effective $CaCO_3$ crystals precipitation taking into consideration the effect of the number of CS flushes was established. It is recommended that the optimum number of CS flushes should be adopted (i.e., 4 CS flushes for high BC concentration of 32 U/mL and two CS flushes for low BC concentration of 8 U/mL) in order to maintain at least 50% of the urea conversion efficiency. In terms of strength improvement, the optimized bio-cemented sand performed better than the OPC treated sand cured at 28 days.

Acknowledgements

The authors would like to acknowledge the contribution of Curtin International Postgraduate Research Scholarship (CIPRS) in supporting this research. The SEM experiments conducted in this research were undertaken using the EM instrumentation (ARC LE130100053) at the John de Laeter Centre, Curtin University.

References

Achal, V., Mukherjee, A., Kumari, D., and Zhang, Q. (2015). "Biomineralization for sustainable construction – A review of processes and applications." *Earth-Science Reviews*, 148, 1-17.

Al-Thawadi, S. M., and Cord-Ruwisch, R. (2012). "Calcium carbonate crystals formation by ureolytic bacteria isolated from Australian soil and sludge." *Journal of Advanced Science and Engineering Research*, 2, 12-26.

Al Qabany, A., and Soga, K. (2013). "Effect of chemical treatment used in MICP on engineering properties of cemented soils." *Géotechnique*, 63(4), 331-339.

Al Qabany, A., Soga, K., and Santamarina, C. (2012). "Factors affecting efficiency of microbially induced calcite precipitation." *Journal of Geotechnical and Geoenvironmental Engineering*, 138(8), 992-1001.

Anbu, P., Kang, C. H., Shin, Y. J., and So, J. S. (2016). "Formations of calcium carbonate minerals by bacteria and its multiple applications." *Springerplus*, 5, 250.

Bosak, T., and Newman, D. K. (2005). "Microbial kinetic controls on calcite morphology in supersaturated solutions." *Journal of Sedimentary Research*, 75, 190-199.

Cheng, L., and Cord-Ruwisch, R. (2014). "Upscaling effects of soil improvement by microbially induced calcite precipitation by surface percolation." *Geomicrobiology Journal*, 31(5), 396-406.

Cheng, L., Cord-Ruwisch, R., and Shahin, M. A. (2013). "Cementation of sand soil by microbially induced calcite precipitation at various degrees of saturation." *Canadian Geotechnical Journal*, 50(1), 81-90.

Cheng, L., Shahin, M. A., and Cord-Ruwisch, R. (2016). "Surface percolation for soil improvement by biocementation utilizing in situ enriched indigenous aerobic and anaerobic ureolytic soil microorganisms." *Geomicrobiology Journal*, 34(6), 546-556.

Cheng, L., Shahin, M. A., and Mujah, D. (2017). "Influence of key environmental conditions on microbially induced cementation for soil stabilization." *Journal of Geotechnical and Geoenvironmental Engineering*, 143(1), 04016083.

Chu, J., Ivanov, V., Naeimi, M., Stabnikov, V., and Liu, H.-L. (2013). "Optimization of calcium-based bioclogging and biocementation of sand." *Acta Geotechnica*, 9(2), 277-285.

DeJong, J. T., Mortensen, B. M., Martinez, B. C., and Nelson, D. C. (2010). "Bio-mediated soil improvement." *Ecological Engineering*, 36(2), 197-210.

Feng, K., and Montoya, B. M. (2016). "Influence of Confinement and Cementation Level on the Behavior of Microbial-Induced Calcite Precipitated Sands under Monotonic Drained Loading." *Journal of Geotechnical and Geoenvironmental Engineering*, 142(1), 04015057.

Gandhi, K. S., Kumar, R., and Ramkrishna, D. (1995). "Some basic aspects of reaction engineering of precipitation processes." *Industrial & Engineering Chemical Research*, 34(10), 3223-3230.

Gomez, M. G., Anderson, C. M., Graddy, C. M. R., DeJong, J. T., Nelson, D. C., and Ginn, T. R. (2016). "Large-scale comparison of bioaugmentation and biostimulation approaches for biocementation of sands." *Journal of Geotechnical and Geoenvironmental Engineering*, 10.1061/(asce)gt.1943-5606.0001640, 04016124.

Ismail, M. A., Joer, H. A., Randolph, M. F., and Meritt, A. (2002a). "Cementation of porous materials using calcite." *Geotechnique*, 52(5), 313-324.

Ismail, M. A., Joer, H. A., Sim, W. H., and Randolph, M. F. (2002b). "Effect of cement type on shear behavior of cemented calcareous soil." *Journal of Geotechnical and Geoenvironmental Engineering*, 128(6), 520-529.

Ivanov, V., and Chu, J. (2008). "Applications of microorganisms to geotechnical engineering for bioclogging and biocementation of soil in situ." *Reviews in Environmental Science and BioTechnology*, 7(2), 139-153.

Jiang, N.-J., and Soga, K. (2017). "The applicability of microbially induced calcite precipitation (MICP) for internal erosion control in gravel–sand mixtures." *Geotechnique*, 67(1), 42-55.

Jiang, N. J., Soga, K., and Kuo, M. (2016). "Microbially induced carbonate precipitation for seepage-induced internal erosion control in sand–clay mixtures." *Journal of Geotechnical and Geoenvironmental Engineering*, 10.1061/(ASCE)GT.1943-5606.0001559.

Martinez, B. C., DeJong, J. T., Ginn, T. R., Montoya, B. M., Barkouki, T. H., Hunt, C., Tanyu, B., and Major, D. (2013). "Experimental optimization of microbial-induced carbonate precipitation for soil improvement." *Journal of Geotechnical and Geoenvironmental Engineering*, 139(4), 587-598.

Mortensen, B. M., Haber, M. J., DeJong, J. T., Caslake, L. F., and Nelson, D. C. (2011). "Effects of environmental factors on microbial induced calcium carbonate precipitation." *Journal of Applied Microbiology*, 111(2), 338-349.

Mujah, D. (2016). "Compressive strength and chloride resistance of grout containing ground palm oil fuel ash." *Journal of Cleaner Production*, 112, 712-722.

Mujah, D., Shahin, M. A., and Cheng, L. (2016a). "Performance of biocemented sand under various environmental conditions." *XVIII Brazilian Conference on Soil Mechanics and Geotechnical Engineering*, Brazilian Society for Soils Mechanics and Geotechnical Engineering, Belo Horizonte.

Mujah, D., Shahin, M. A., and Cheng, L. (2016b). "State-of-the-art review of bio-cementation by microbially induced calcite precipitation (MICP) for soil stabilization." *Geomicrobiology Journal*, 34(6), 524-537.

Nakarai, K., and Yoshida, T. (2015). "Effect of carbonation on strength development of cement-treated Toyoura silica sand." *Soils and Foundations*, 55(4), 857-865.

Okwadha, G. D., and Li, J. (2010). "Optimum conditions for microbial carbonate precipitation." *Chemosphere*, 81(9), 1143-1148.

Park, K., Jun, S., and Kim, D. (2014). "Effect of strength enhancement of soil treated with environment-friendly calcium carbonate powder." *Scientific World Journal*, 2014, 526491.

Schnaid, F., Prietto, P. D. M., and Consoli, N. C. (2001). "Characterization of cemented sand in triaxial compression." *Journal of Geotechnical and Geoenvironmental Engineering*, 127(10), 857-868.

Shahrokhi-Shahraki, R., O'Kelly, B. C., Niazi, A., and Zomorodian, S. M. A. (2015). "Improving sand with microbial-induced carbonate precipitation." *Proceedings of the ICE - Ground Improvement*, 168(3), 217-230.

Terzis, D., Bernier-Latmani, R., and Laloui, L. (2016). "Fabric characteristics and mechanical response of bio-improved sand to various treatment conditions." *Géotechnique Letters*, 6(1), 50-57.

van Paassen, L. A. (2009). "Biogrout: Ground improvement by microbially induced carbonate precipitation." PhD Thesis, Delf University of Technology, Netherlands.

van Paassen, L. A., Daza, C. M., Staal, M., Sorokin, D. Y., van der Zon, W., and van Loosdrecht, M. C. M. (2010). "Potential soil reinforcement by biological denitrification." *Ecological Engineering*, 36(2), 168-175.

Whiffin, V. S. (2004). "Microbial CaCO3 precipitation for the production of biocement." PhD Thesis, Murdoch University, Australia.

Whiffin, V. S., van Paassen, L. A., and Harkes, M. P. (2007). "Microbial carbonate precipitation as a soil improvement technique." *Geomicrobiology Journal*, 24(5), 417-423.

Yasuhara, H., Neupane, D., Hayashi, K., and Okamura, M. (2012). "Experiments and predictions of physical properties of sand cemented by enzymatically-induced carbonate precipitation." *Soils and Foundations*, 52(3), 539-549.

Table 1. Properties of sand used in the current study

Property	Value
D_{10} (mm)	0.17
D_{30} (mm)	0.21
D_{60} (mm)	0.28
C_u	1.65
C_c	0.84
G_s	2.71
$e_{\min}$	0.48
$e_{\max}$	0.71
OMC (%)	12
$\gamma_{d\text{-}max}$ (kN/m3)	16.3
η (%)	40
k ($\times 10^{-5}$ m/s)	80 ± 0.5
USCS classification	SP

OMC = optimum moisture content; $\gamma_{d\text{-}max}$ = maximum dry density; η = porosity; k = permeability.

Table 2. Bacteria culture and cementation solution recipes used in the current study

	Bacteria culture		Cementation solution		
ID	Biomass concentration (OD_{600} (cell density, g/L))*	Urease concentration (U/mL)	Urea (g/L)	Calcium chloride dehydrate (g/L)	Molarity (M)
1	1.24 (0.543)	8.33	15.1	36.75	0.25
2	2.36 (1.033)	16.25	30.1	73.5	0.5
3	4.46 (2.399)	32.15	60.2	147	1

*The OD_{600} and cell density follows the equation: C (biomass density, g/L) = 0.438 × OD (600 nm) (R^2 = 0.998).

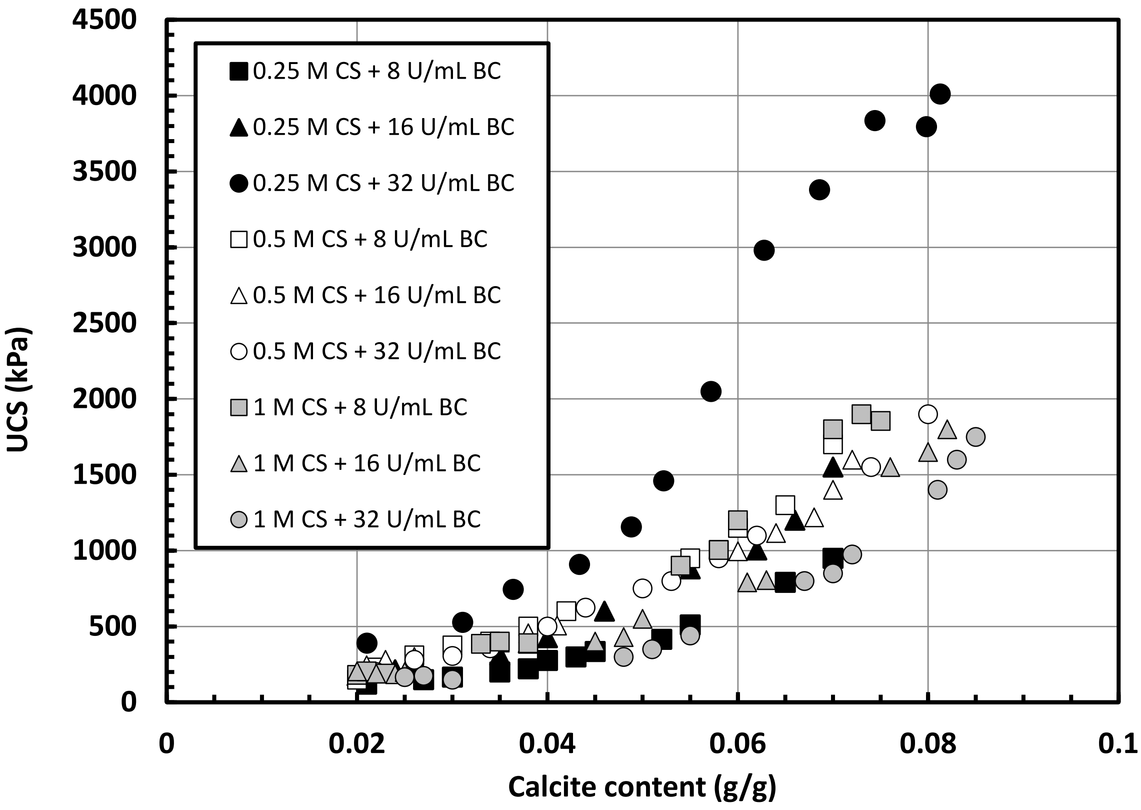

Fig. 1. Effect of different BC concentrations on the strength of bio-cemented sand samples at various CS concentrations.

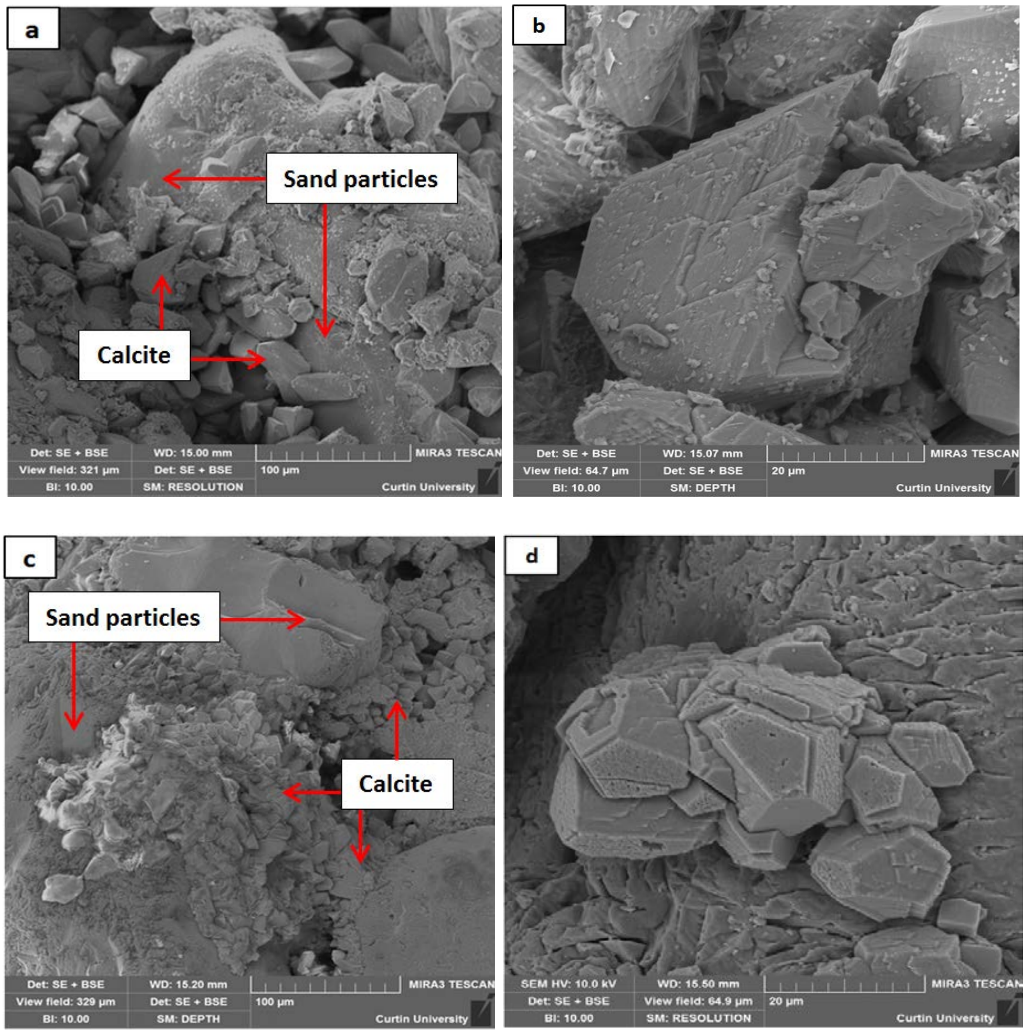

Fig. 2. Microstructure of soil samples (0.05 g/g $CaCO_3$) content treated with different concentrations of BC and CS, including high BC (32 U/mL) and low CS (0.25 M) concentrations (a & b) and high BC (32 U/mL) and high CS concentrations (1 M) (c & d).

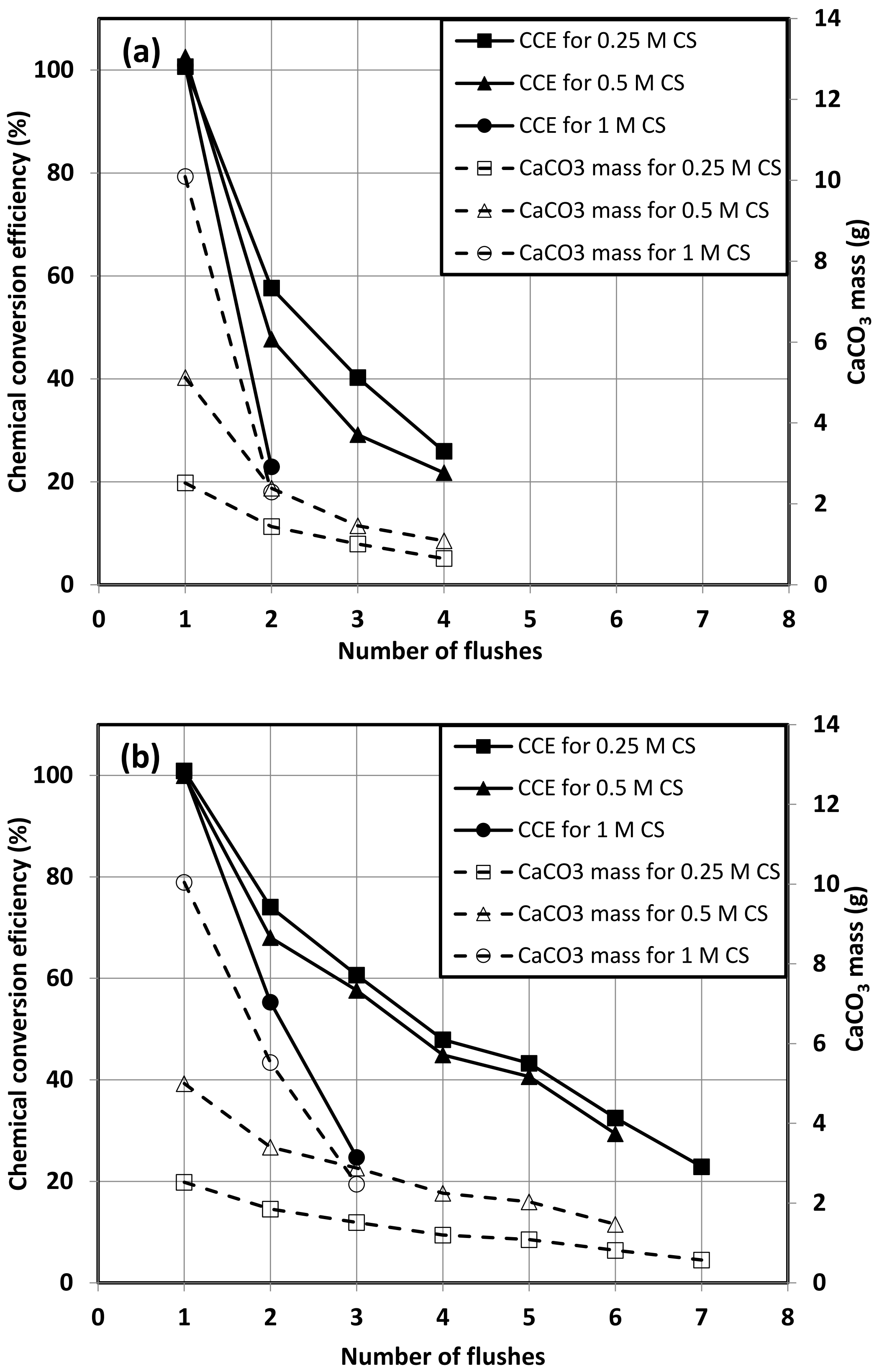

Fig. 3. Effect of number of CS flushes on the ammonia conversion efficiency in the MICP process: (a) 8 U/mL BC; and (b) 32 U/mL BC.

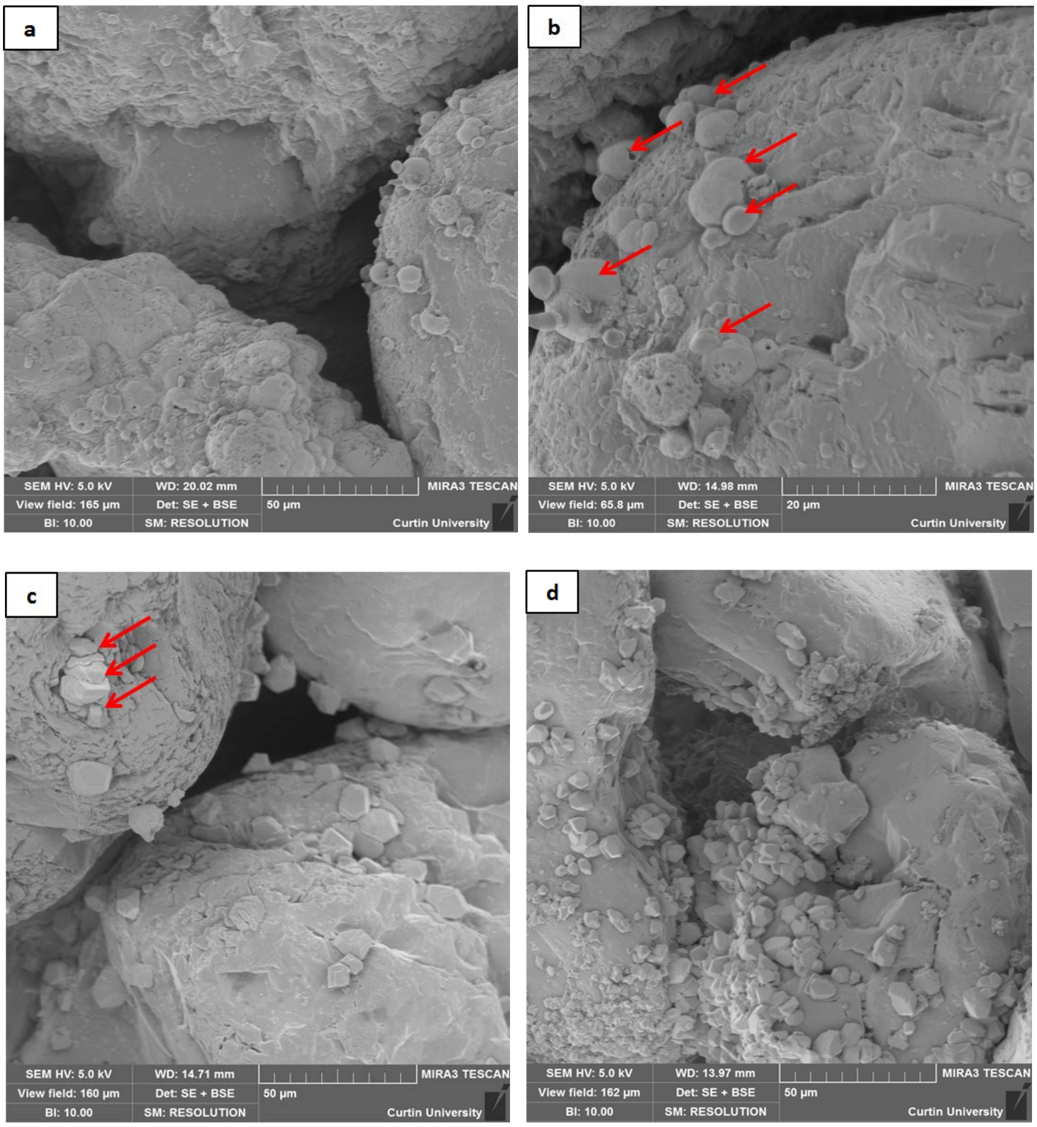

Fig. 4. Evolution of effective $CaCO_3$ crystals precipitation: (a) CS flushing induces the development of MICP process in the nucleation sites (image taken after one full void volume of CS injection); (b) formation of metastable primary spherical shaped precipitates; (c) crystal growth indicated by the red arrows showing the cluster of single crystal creating mesocrystals which successively form the effective $CaCO_3$ crystals (image taken after two full void volume of CS injection); and (d) precipitation of the effective $CaCO_3$ crystals concentrated at the soil pore throat (image taken after three full void volume of CS injection).

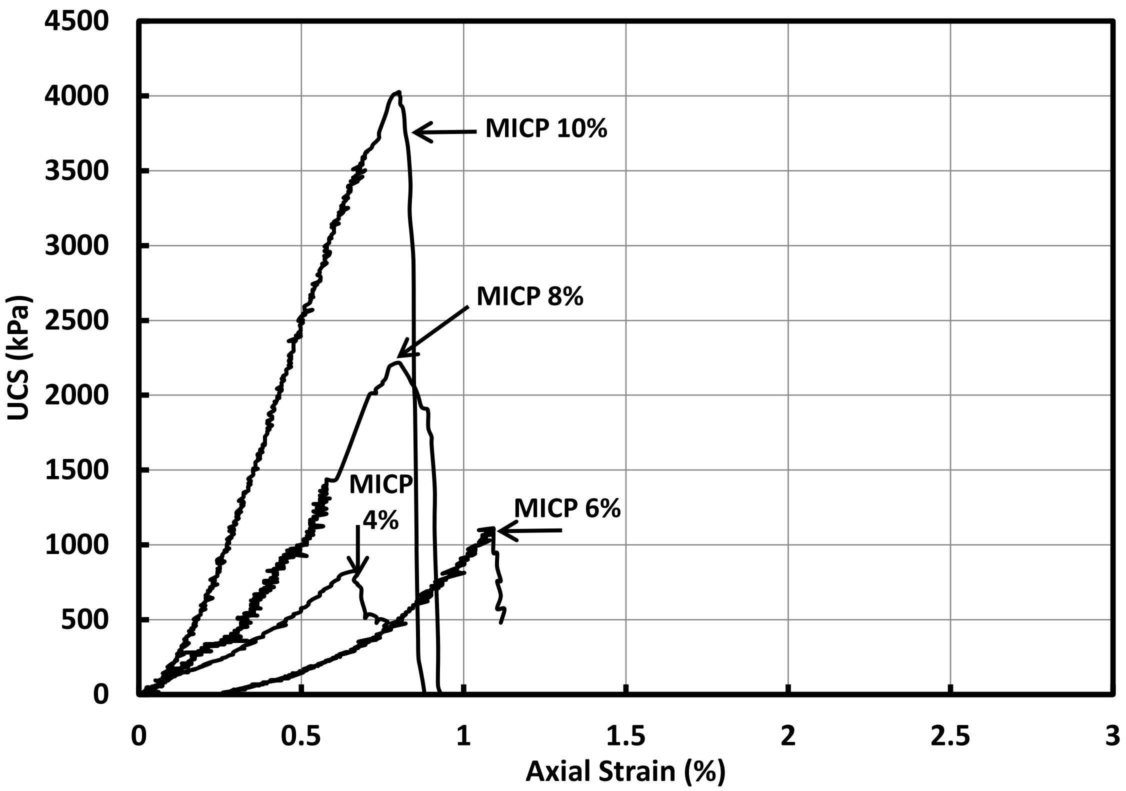

Fig. 5. Stress-strain relationships of optimum MICP treated samples (32 U/mL BC and 0.25 M CS).

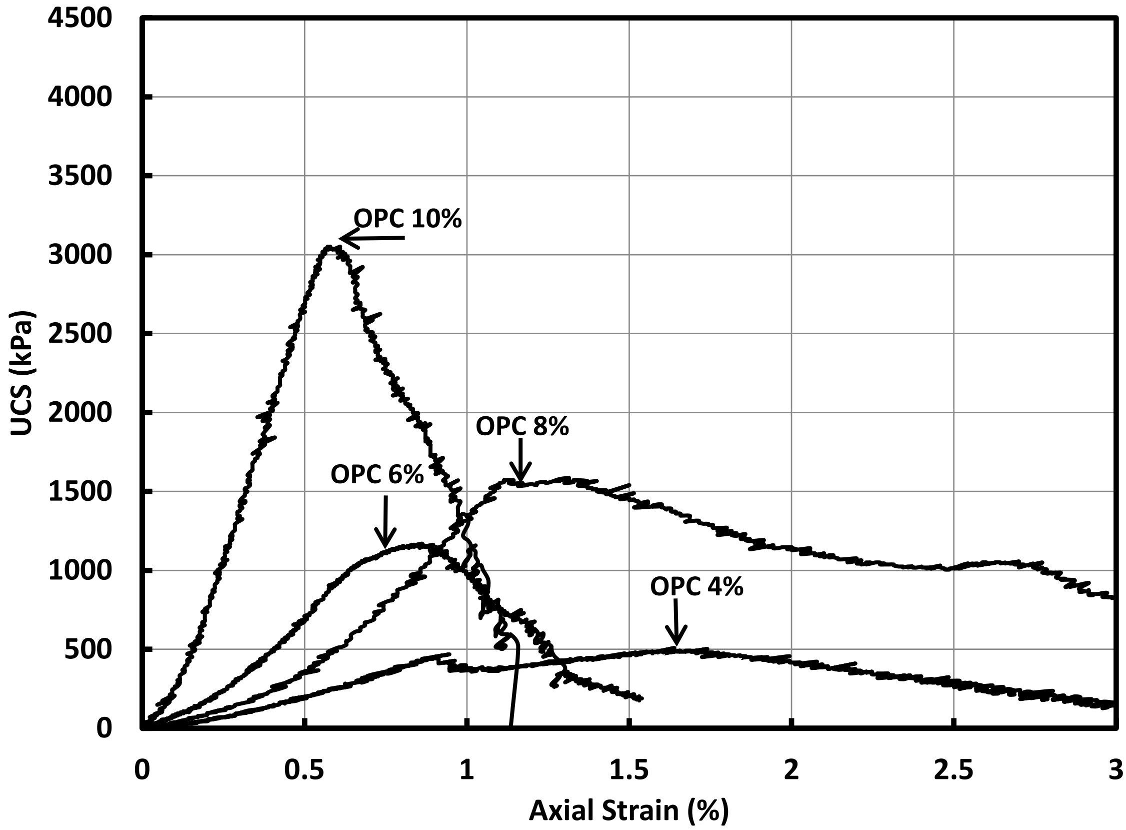

Fig. 6. Stress-strain relationships of OPC samples treated at 28 days.

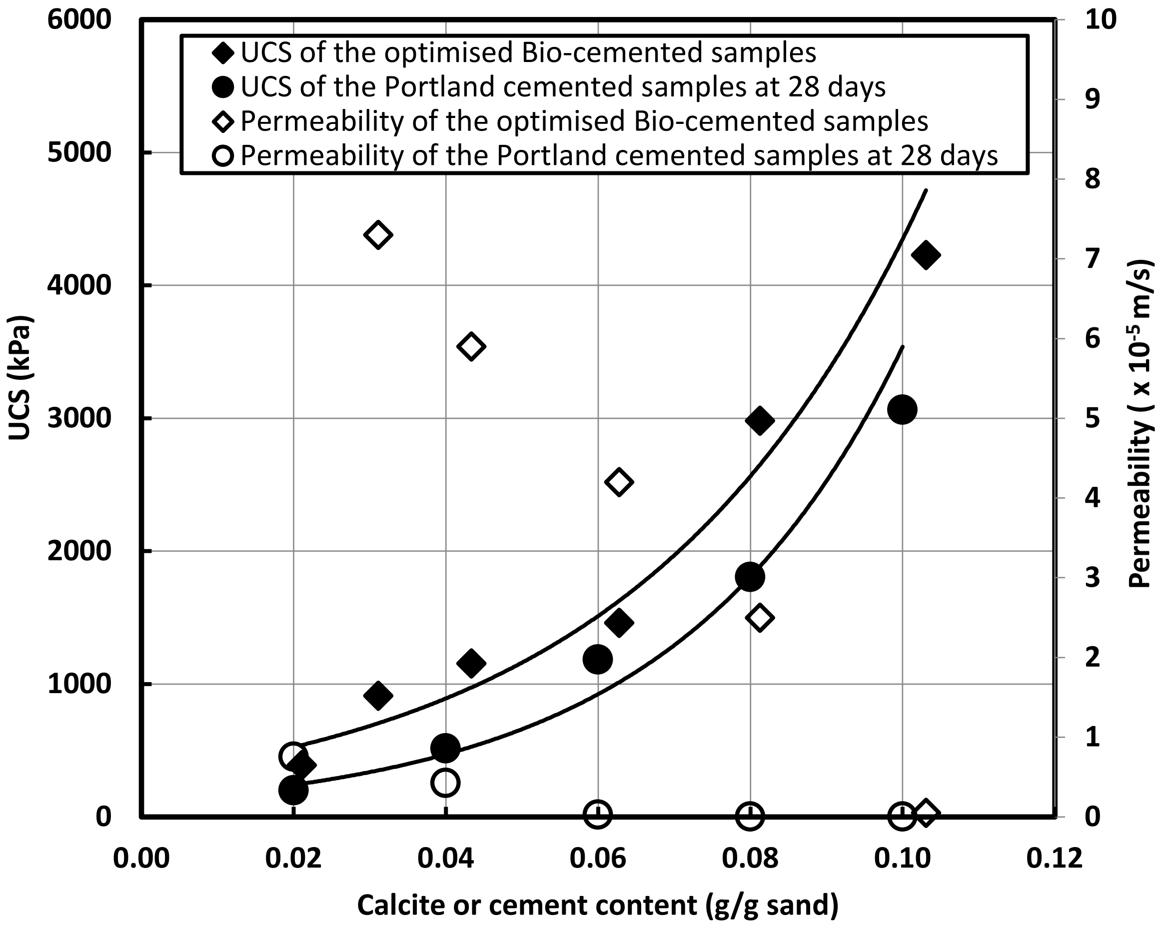

Fig. 7. Comparison of UCS and permeability of optimized bio-cemented (32 U/mL BC and 0.25 CS) and OPC treated sands.

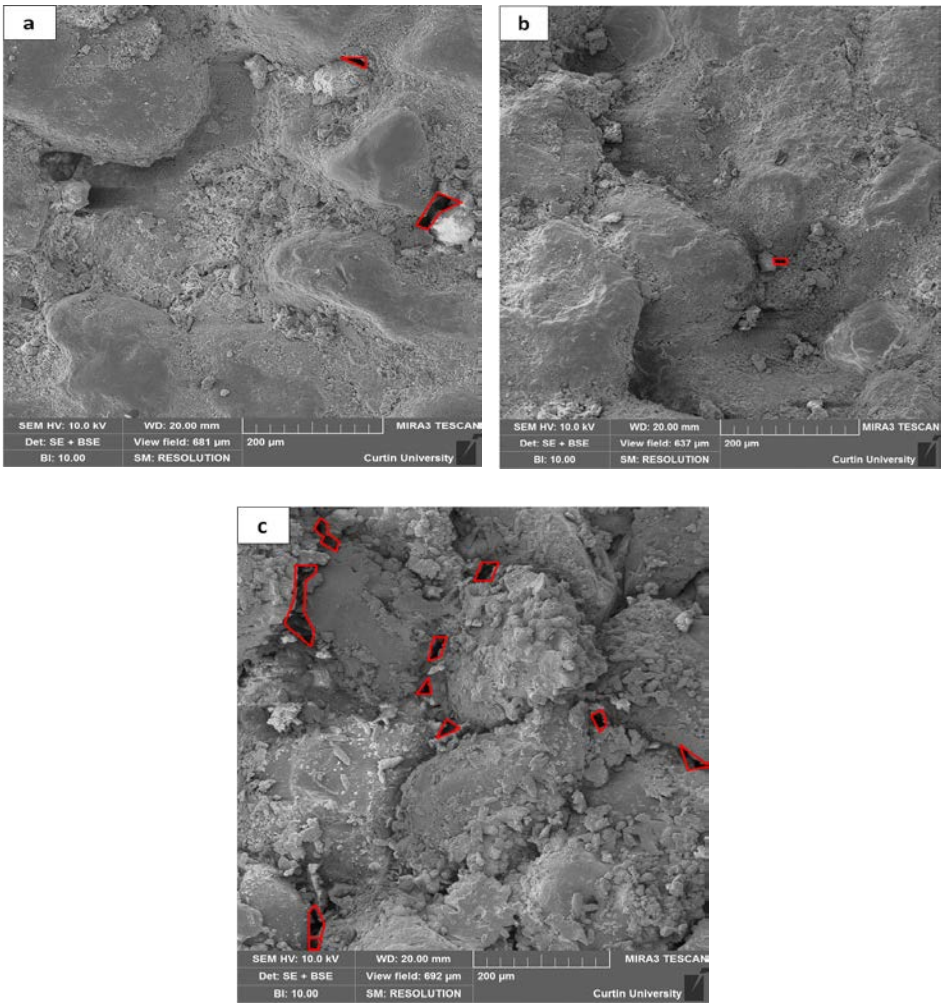

Fig. 8. SEM images showing the effect of cement content on permeability: (a) formation of C-S-H gel in the OPC treated sample (at 7 days) for 8% cement content; (b) formation of C-S-H gel in the OPC treated sample (at 28 days) for 8% cement content; and (c) precipitation of the effective $CaCO_3$ crystals in the bio-cemented sample at 8% $CaCO_3$ content.